Propofol Reduces Epithelial to Mesenchymal Transition, Invasion and Migration of Gastric Cancer Cells through the MicroRNA-195-5p/Snail Axis

Authors' Contribution:
Study Design A
Data Collection B
Statistical Analysis C
Data Interpretation D
Manuscript Preparation E
Literature Search F
Funds Collection G

ABCDE 1 Fenghua Liu*
ABDE 1 Fengyu Qiu*
DF 1 Min Fu
BCDF 1 Huayong Chen
BCDF 2 Hui Wang

1 Department of Anesthesiology, Yidu Central Hospital, Weifang, Shandong, P.R. China
2 Operating Room, Affiliated Hospital of Weifang Medical University, Weifang, Shandong, P.R. China

Corresponding Author:
Source of support:

* Fenghua Liu and Fengyu Qiu contributed equally to this work
Hui Wang, e-mail: wanghui081202@163.com
Departmental sources

Background: Gastric cancer (GC) is a life-threating malignancy worldwide. Accumulating studies suggest propofol has anti-tumor functions in addition to the anesthetic effect. This study aimed to figure out the effects of propofol treatment in GC development.

Material/Methods: Human GC SGC-7901 and NCI-N87 cells were treated with different doses of propofol. Then the invasion and migration of GC cells was measured. SGC-7901 cells following 10 µM propofol treatment were applied in the following experiments. MicroRNAs (miRNAs) with differential expression in cells with or without propofol treatment were analyzed. Expression of miR-195-5p, Snail, vimentin and E-cadherin in SGC-7901 cells was measured, and then loss-of-function of miR-195-5p and gain-of-function of Snail were performed. Target relation between miR-195-5p and Snail was confirmed using luciferase assay. Xenograft tumor was induced in nude mice to identify the effect of propofol on GC *in vivo*.

Results: Propofol reduced epithelial to mesenchymal transition (EMT), invasion and migration of GC cells in a dose-dependent manner. Propofol elevated miR-195-5p expression but reduced Snail expression, and it reduced vimentin but increased E-cadherin expression in SGC-7901 cells. miR-195-5p directly bound to Snail. miR-195-5p inhibition or Snail promotion reversed propofol-inhibited malignant behaviors of SGC-7901 cells. *In vitro* results were reproduced in *in vivo* experiments.

Conclusions: Our study found that propofol could inhibit EMT, invasion, and migration of GC cells by promoting miR-195-5p expression and suppressing Snail expression. This study may provide novel insights in GC treatment.

MeSH Keywords: Neoplasm Metastasis • Propofol • Snails • Stomach Neoplasms

Full-text PDF: https://www.medscimonit.com/abstract/index/idArt/920981

3347   1   5   39

Background

Gastric cancer (GC) is one of the most prevailing and life-threatening cancers around the world [1,2]. The incidence of GC is reported higher in developing countries in South America, Eastern Asia, and Central and Eastern Europe than that in developed nations, with approximately 70% GC cases are found in developing nations around the world [3]. China represents 25% of all GC death cases, with the 5-year survival rate at 40% since most GC patients were diagnosed at advanced stages [4]. As a heterogeneous disease, GC is thought to be a complicated illness with diverse influence factors such as environment, lifestyle, dietary intake of salt, genetics, vitamin C and *Helicobacter pylori* infection [3]. Despite the improvements in radiotherapy, chemotherapy and operation techniques for GC in the past few years, the overall survival rate of GC patients is unfavorable owing to the resistance to traditional therapies, recurrence and metastasis [5–7]. Thus, identifying the regulatory mechanisms and developing novel therapeutic options for GC is of great importance.

Recently, the use of anesthetics has aroused wide concerns in cancer therapy, since anesthetics may result in improved outcomes during cancer resection, but the volatile anesthetics may also lead to tumor growth and metastasis [8,9]. Propofol is an anesthetic agent that is widely applied in most kinds of surgeries due to the short effect and quick recovery [10]. Aside from its anesthetic effects, propofol holds other functions including anti-tumor attributes [11]. Besides, propofol has been documented to inhibit the survival and growth of GC cells *in vitro* [12], but the mechanisms are not fully understood. Importantly, propofol has been documented to show anti-tumor activity with the involvement of multiple microRNAs (miRNAs) [8,13]. miRNAs are well known to prevent translation and expression of target genes via binding to the 3'untranslated regions (3'UTRs) of mRNAs [14]. miRNAs exert key functions in diverse cellular biological processes such as proliferation, migration, and epithelial to mesenchymal transition (EMT) [15]. Here, we analyzed the miRNAs with differential expression before and after propofol treatment with microarrays and analyzed the aberrantly expressed miRNAs in GC patients, with miR-195-5p was found to have the potential to affect GC progression. Given that dysregulation of miR-195-5p has been identified to involve in the development of several cancers [16,17]. The role of miR-195-5p in GC and the downstream mechanisms were probed.

As aforementioned, miRNAs play significant roles in cell EMT, invasion and migration. EMT is crucial for tumorigenesis and tumor development. During oncogenesis processes, normal epithelial cells develop to carcinoma *in situ* through EMT, and the cancer cells *in situ* can further invade and migrate into lymph vessels or blood vessels through EMT for remote metastasis [18–20].The zincfinger protein transcription factor Snail is well-known for its role in promoting EMT process and enhancing the invasion of tumor cells via promoting the E-cadherin-to-N-cadherin shift [21]. A previous study noted that Snail may have a clinical significance in the progression of GC [22]. Based on the discussion above, we hypothesized that propofol might play roles in GC progression with the involvement of miR-195-5p and Snail, and both *in vivo* and *in vitro* experiments were performed to validate the hypothesis.

Material and Methods

Ethics statement

This study gained the approval of the Clinical Ethical Committee of Yidu Central Hospital. All procedures were performed carefully to minimize the pain of conscious animals.

Cell culture and transfection

Human GC cell lines SGC-7901 and NCI-B87 (Shanghai Institute of Biochemistry and Cell Biology, Chinese Academic of Science, Shanghai, China) were cultivated in 10% Dulbecco's Modified Eagle's Medium (DMEM) (Hyclone Company, Logan, UT, USA) containing 10% fetal bovine serum (FBS) at 37°C with 5% CO_2. Cells were detached with trypsin and passaged once every 2 or 3 days. Then the SGC-7901 and NCI-B87 cells in the logarithmic growth period were treated with 5 µM propofol (Sigma-Aldrich, Merck KGaA, Darmstadt, Germany) (P5 group), 10 µM propofol (P10 group), and 20 µM propofol (P20 group), and cells were collected for following experiments 72 hours after propofol treatments. Another batch of 10 µM propofol-treated SGC-7901 cells were allocated into the blank group (without transfection), the inhibitor-negative control (NC) group (transfected with inhibitor NC), the miR-195-5p inhibitor group (transfected with miR-195-5p inhibitor), the pc group (transfected with pcDNA3.1), and the pc-Snail group (transfected with pcDNA3.1-Snail). All transfections were conducted with Lipofectamine™ 2000 reagent (Invitrogen Inc., Carlsbad, CA, USA), with the transfection efficiency detected using reverse transcription quantitative polymerase chain reaction (RT-qPCR) and western blot analysis 48 hours after transfections. The inhibitor-NC, miR-195-5p inhibitor, pcDNA3.1 and pcDNA-3.1-Snail were acquired from Thermo Fisher Scientific Inc. (Waltham, MA, USA).

Microarray analysis

Total RNA from SGC-7901 cells and 10 µM propofol-treated SGC-7901 cells was extracted using a TRIzol kit (Invitrogen). Then the miRNAs were separated using Ambion's miRNA Isolation Kit (Invitrogen), and the miRNA microarrays were

Table 1. Primer sequences for RT-qPCR.

Gene	Sequence
miR-1827	F: 5'-ACTAGTTATAACCCTAGGAATTTAGACAACC-3'
	R: 5'-AAGCTTACATCATTACTCCCATCCCTTAC-3'
miR-195-5p	F: 5'-CTGGAGCAGCACAGCCAATA-3'
	R: 5'-AGCTTCCCTGGCTCTAGCA-3'
miR-96-5p	F: 5'-AAGCTTACATCATTACTCCCATCCCTTAC-3'
	R: 5'-CCGGAATTCATCTGCTGGCCCAGCTCAGATTG-3'
miR-93-5p	F: 5'-ACACTCCAGCTGGGTCCTGTACTGAGCTGCCC-3'
	R: 5'-CTCAACTGGTGTCGTGGA-3'
miR-106b-5p	F: 5'-TGCGGCAACACCAGTCGATGG-3'
	R: 5'-CCAGTGCAGGGTCCGAGGT-3'
U6	F: 5'-CTCGCTTCGGCAGCACA-3'
	R: 5'-AACGCTTCACGAATTTGCGT-3'
Snail1	F: 5'-TATGCTGCCTTCCCAGGCTTG-3'
	R: 5'-ATGTGCATCTTGAGGGCACCC-3'
GAPDH	F: 5'-GGTGGTCTCCTCTGACTTCAACA-3'
	R: 5'-GTTGCTGTAGCCAAATTCGTTGT-3'

RT-qPCR – reverse transcription quantitative polymerase chain reaction; miR – microRNA; GAPDH – glyceraldehyde-3-phosphate dehydrogenase.

labeled, hybridized and washed as per the instructions of a miRCU RY™ Array kit (Invitrogen). After washing and drying, the miRNA microarrays were scanned on a Genepxi 4000B dual-channel laser image scanner (Molecular Devices, CA, USA) at the single wavelength of 635 nm. Then the results were analyzed.

RT-qPCR

Total RNA from SGC-7901 cells was extracted and reversely transcribed to cDNA, with the primers synthesized by Guangzhou RiboBio Co., Ltd. (Guangzhou, Guangdong China). RT-qPCR was conducted as per the protocol of the SYBR Premix Ex Tap (Toyobo Co., Ltd., Kitaku, Osaka, Japan). The $2^{-\Delta\Delta Ct}$ method was used to measure the relative expression of target genes. U6 and glyceraldehyde-3-phosphate dehydrogenase (GAPDH) were applied as the internal references. The primers are shown in Table 1.

Western blot analysis

Total proteins were extracted from SGC-7901 cells with the protein concentration assessed. Next, the proteins were added with loading buffer and run on sodium dodecyl sulfate-poly-acrylamide gel electrophoresis (SDS-PAGE), and then transferred

onto PVDF membranes. The membranes were sealed with 50 g/L skimmed milk for 1 hour, washed with tris-saline buffer with 0.1% tween 20 (TBST), and then cultured with the primary antibodies Snail (ab180714, 1: 1000), vimentin (ab8978, 1: 1000) and E-cadherin (ab76055, 1: 1000) (all purchased from Abcam Inc., Cambridge, UK) at 4°C overnight. Next, the membranes were cultured with secondary antibody immunoglobulin G (ab6728; 1: 2000, Abcam) for 1 hour at room temperature after TBST washes. Thereafter, the membranes were washed again, added with enhanced chemiluminescence reagent, exposed in a dark room, visualized and fixated for observation. GAPDH (ab8245, 1: 1000) was set as the internal reference, and the images were analyzed using ImageJ 2×software (v2.1.4.7, Rawak Software, Inc., Stuttgart, Germany)

Transwell assays

Cell migration and invasion were assessed via Transwell assays. Regarding migration assay, the Transwell chambers were placed into 24-well plates, and the cells were resuspended in DMEM to 1×10^5 cells per mL. Each basolateral chamber was added with 800 μL DMEM containing 10% FBS, while the apical chamber was added with 200 μL cell suspension. The medium was absorbed after 24 hours of incubation at 37°C. Migrated cells were fixed with 5% glutaraldehyde for 30 minutes and then subjected to 20 minutes of crystal violet staining. Cells in the apical chamber were removed, and then the plates were dried and observed under a microscope for cell calculation, with 5 fields randomly selected. Regarding invasion assay, the apical chamber was pre-coated with Matrigel, and each well was added with 1×10^5 cells. After 24 hours of regular incubation, the Matrigel in the apical chamber was wiped away. Then the plates were fixed in 750 mL/L alcohol for 15 minutes, stained with crystal violet for 20 minutes, repeatedly washed with phosphate buffer saline (PBS) to wash away the remaining staining liquid. Then the plates were observed under a microscope with 5 fields randomly selected.

Dual luciferase reporter gene assay

A computer-based program (*http://starbase.sysu.edu.cn/index. php*) was applied to predict the binding relation in miR-195-5p and Snail. The 3'UTR sequence of Snail containing the binding sites with miR-195-5p was inserted into the pGL2-Basic Vector (Promega, Madison, WI, USA) to construct Snail 3'UTR wild type (Snail-WT) plasmid, and the corresponding Snail 3'UTR mutant (Snail-MUT) plasmid was constructed as well. HEK-293T cells (Shanghai Yeasen Biotechnology Co., Ltd., Shanghai, China) were incubated in DMEM supplemented with 10% FBS, 1% penicillin, and streptomycin at 37°C with 5% CO_2. After detached by trypsin, the cells were subcultured once every 2nd or 3rd day. Well-constructed Snail-WUT and Snail-WT plasmids were mixed with miR-195-5p mimic or mimic NC, respectively,

and transfected into 293T cells using Lipofectamine™ 2000. Then the luciferase activities were detected.

Immunofluorescence staining

SGC-7901 cells were sorted into 24-well plates at 2×10^4 cells/well. Cells grew on slides for 24 hours. Then the cell slides were washed with PBS (3 times for 5 minutes each time), fixed in 4% polyformaldehyde for 15 minutes, washed with PBS again (3 times for 5 minutes each time), and sealed with goat serum for 30 minutes. Then the sealing liquid was absorbed, and the cells were cultivated with the primary antibody E-cadherin (ab76055, 1: 1000) at 4°C overnight. Next, the slides were washed with PBS containing 0.05% (v/v) Tween-20 (PBST) 3 times for 3 minutes each time, and then incubated with the diluted fluorescence (Cy3)-labeled goat anti-rabbit IgG (Boster Biological Technology Co., Ltd., Hubei, China) in a wet box at 20–37°C for 1 hour with the remaining liquid absorbed. Then the slides were further washed with PBST 3 times for 3 minutes each time, and treated with 4',6-diamidino-2-phenylindole (DAPI, Shanghai Beyotime Biotechnology Co., Ltd., Shanghai, China) in the dark for 5 minutes to stain the nuclei. The remaining DAPI was washed away with PBST 4 times for 5 minutes each time; then the slides were sealed with mounting medium containing fluorescent mounting media. Finally, the staining was photographed under a fluorescence microscope (BX53, Olympus Optical Co., Ltd., Tokyo, Japan).

Xenograft tumor in nude mice

Fifteen nude mice (4 weeks old, 15–18 g, strain: BALB/c nude) were purchased from Haisco Pharmaceutical Group (Chengdu, Sichuan, China) (License No. SYXK (Sichuan) 2018-182). SGC-7901 cells were trypsinized and centrifuged with the supernatant discarded. Then the cells were resuspended in PBS till the cell concentration to 1×10^7/mL. Next, 200 µL cell suspension was subcutaneously injected into the right hind leg of nude mice. Ten days later, subcutaneous tubercles about 5 mm in diameter were found in the 15 nude mice, which indicated successful GC model establishment. Next, the nude mice were numbered by weight and allocated into 3 groups, 5 mice for each group. The 3 groups of mice were intraperitoneally injected with equal volume of saline, 5 µM propofol and 20 µM propofol once every 5 days, respectively. The tumor volume was evaluated using a Vernier caliper, and the mice were sacrificed via cervical dislocation at the 25th day, after which the tumor weight was evaluated.

Measurement of the xenograft tumor migration

SGC-7901 cells were trypsinized and centrifuged. Then the cells were resuspended with PBS to adjust the cell concentration to 4×10^5/mL. Twelve nude mice (4 weeks old, 15–18 g)

were numbered by weight and assigned into 3 groups into 2 groups, 6 mice for each group. The mice were injected with 200 µL cell suspension through the caudal vein. One day after successful GC model establishment, the 2 groups of mice were intraperitoneally injected with equal volume of saline or 20 µM propofol once every 5 days, respectively. The mice were observed every day and sacrificed via cervical dislocation at the 35th day. Then the liver and lung tissues were separated, fixed in formalin for 24 hours, embedded with paraffin, and cut into sections.

Hematoxylin and eosin (H&E) staining

The paraffin-embedded sections were dewaxed, and then soaked in gradient concentrations of alcohol (5 minutes for each concentration) and in water for 10 minutes. After the water absorbed and air dried, the sections were subjected to 5 minutes of hematoxylin staining, soaked in hydrochloric ethanol for 10 seconds, washed with clean water, and turned blue in 60°C warm water for 10 minutes. Next, the sections were stained with eosin for 1 minute, sealed with neutral balsam after air dried, and then observed under a microscope.

Statistical analysis

Data were analyzed using SPSS 21.0 (IBM Corp. Armonk, NY, USA). Measurement data are normally distributed and expressed as mean±standard deviation. The t-test was applied for comparisons between 2 groups, while one-way analysis of variance (ANOVA) or 2-way ANOVA for multi-groups, and Tukey's multiple comparisons test for post hoc test. P value was obtained by 2-tailed test, and $P < 0.05$ meant statistical differences.

Results

Propofol inhibited EMT, invasion and migration of GC cells

After propofol treatments, the Snail and vimentin levels reduced while the E-cadherin level increased in SGC-7901 cells (all $P < 0.01$), with higher propofol concentrations leading to more significant changes (Figure 1A). Similar trends were found in NCI-N87 cells after propofol treatments ($P < 0.01$) (Figure 1B). The immunofluorescence assay result identified that E-cadherin protein was located on cell membrane in SGC-7901 and NCI-N87 cells (Figure 1C). Meanwhile, compared to the untreated SGC-7901 cells, 5 µM propofol treatment reduced the number of invaded and migrated cells ($P < 0.05$), while this inhibition was further improved when the propofol concentration was increased ($P < 0.01$) (Figure 1D). The same trends were found in NCI-N87 cells (Figure 1E, 1F).

Upregulation of miR-195-5p was responsible for propofol-suppressed EMT, invasion and migration of GC cells

To explore the potential mechanism involved in the propofol-suppressed EMT, invasion and migration of GC cells, we investigated the differentially expressed miRNAs in the SGC-7901 cells with or without 10 µM propofol treatment via microarray

analysis. The results suggested that miR-195-5p was upregulated in SGC-7901 cells after 10 µM propofol treatment (Figure 2A). The miRNAs with differential expression after 10 µM propofol treatment were further detected using RT-qPCR, and 5 miRNAs were found upregulated, among which miR-195-5p presented a significant increase (Figure 2B). Meanwhile, the online software (http://starbase.sysu.edu.cn/panMirDiffExp.php) predicted
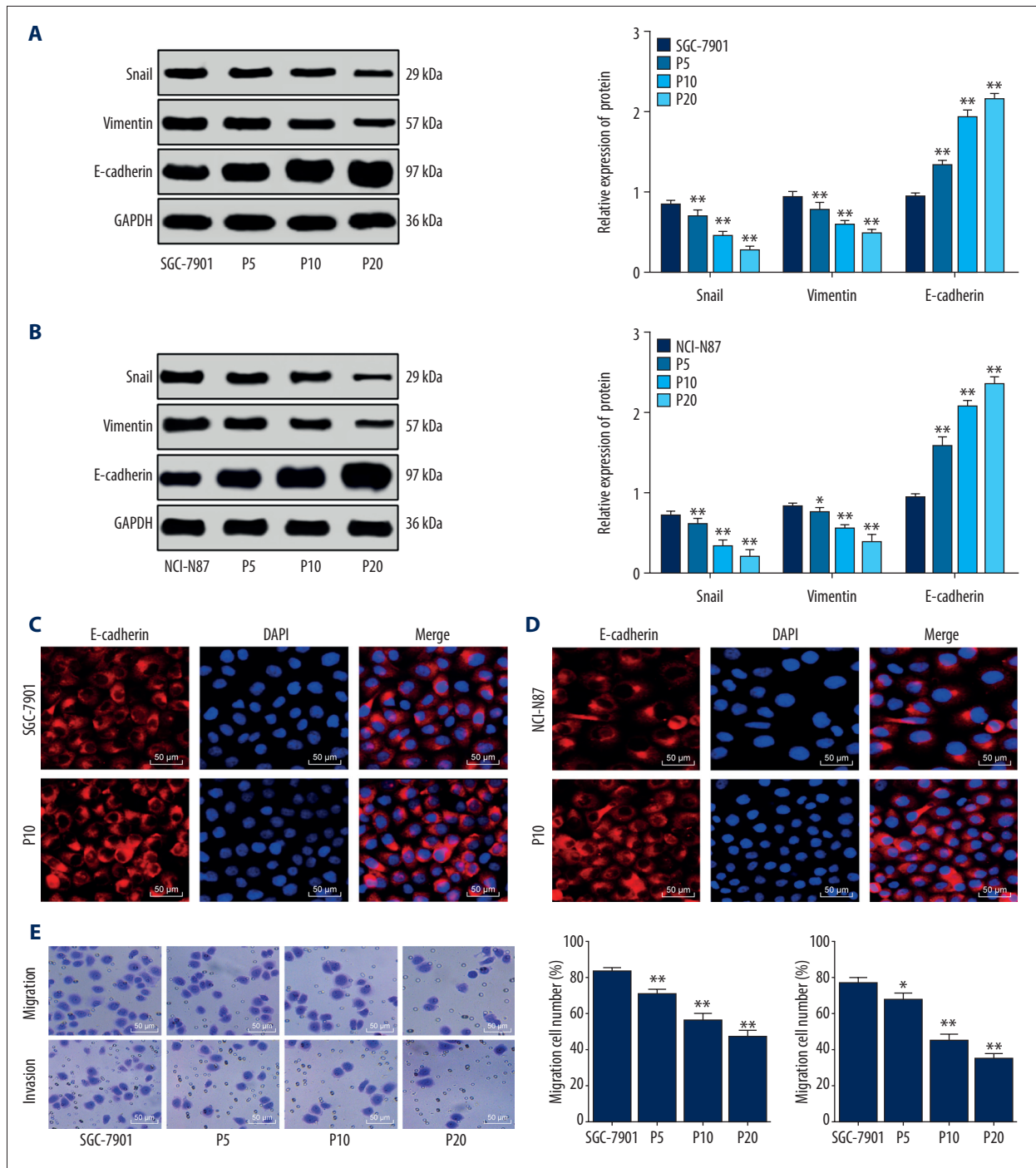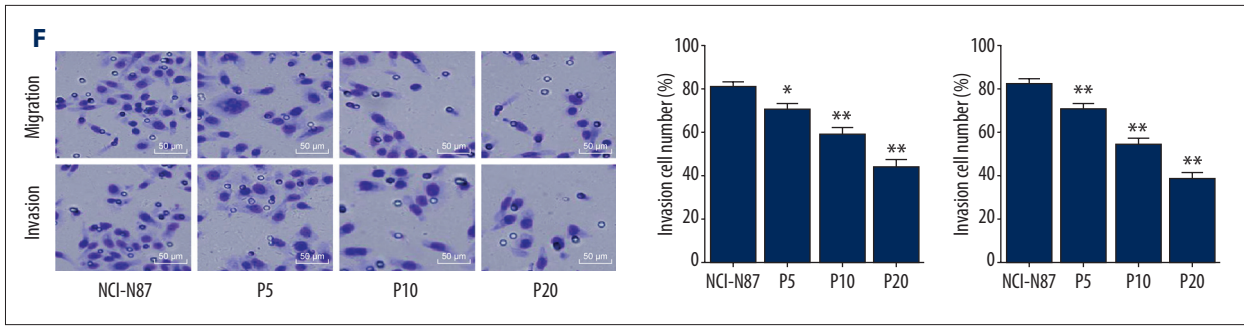
Figure 1. Propofol inhibits EMT, invasion and migration of GC cells. (**A, B**) Protein levels of Snail, vimentin and E-cadherin in SGC-7901 (**A**) and NCI-N87 (**B**) cells detected using western blot analysis. (**C, D**) Protein levels of E-cadherin in SGC-7901 (**C**) and NCI-N87 (**D**) cells measured using immunofluorescence staining (200×). (**E, F**) Migration and invasion of SGC-7901 (**E**) and NCI-N87 cells (**F**) detected using Transwell assays. In panel **A** and **B**, data were analyzed using 2-way ANOVA, while in panel **E** and **F**, data were analyzed using one-way ANOVA, and Tukey's multiple comparisons test was applied for post hoc test; in panels **A** and **E**, *, compared to the SGC-7901 group, while in panels **B** and **F**, *, compared to the NCI-N87 group, * $P<0.05$; ** $P<0.01$; repetition=3. EMT – epithelial to mesenchymal transition; GC – gastric cancer.
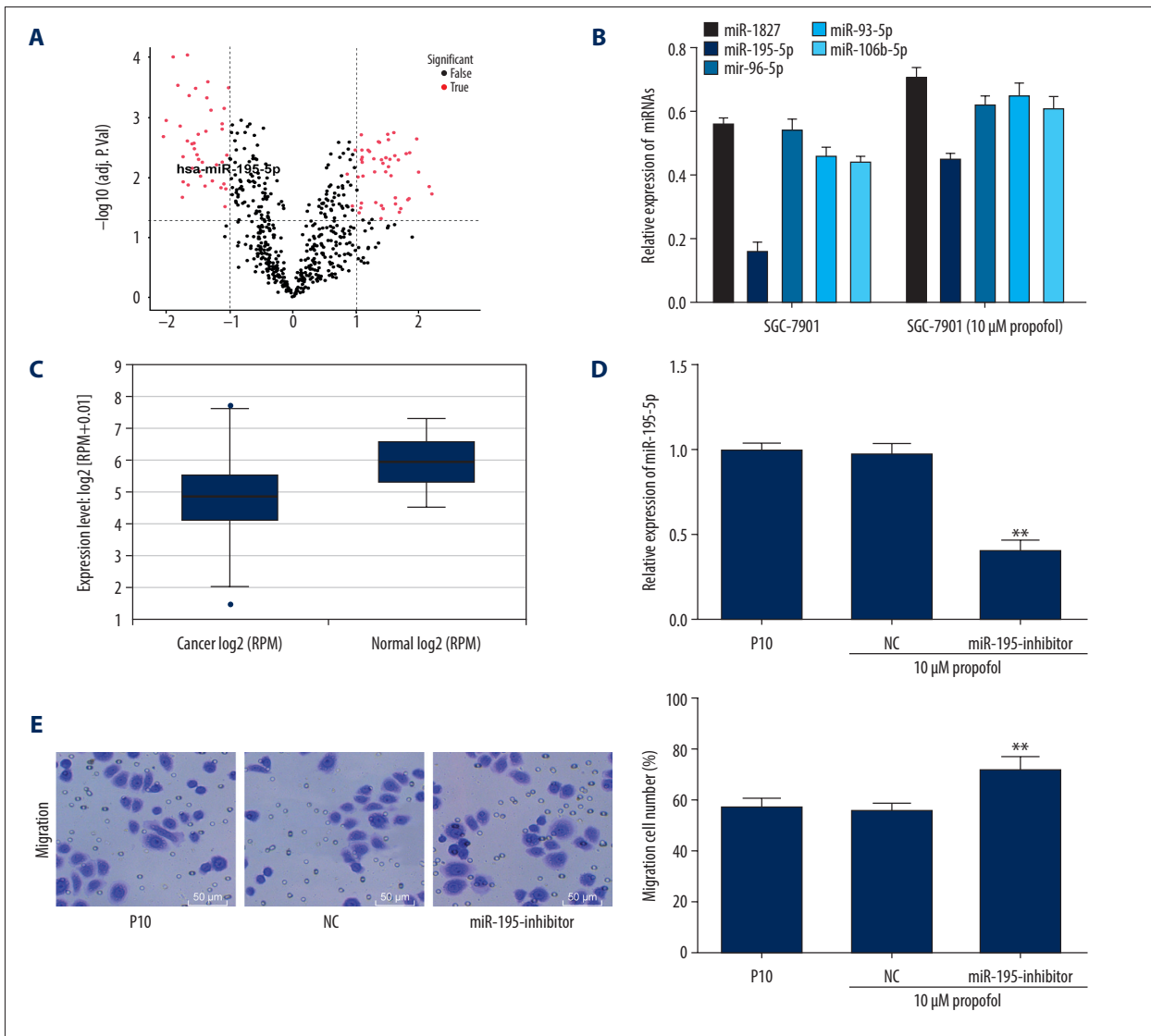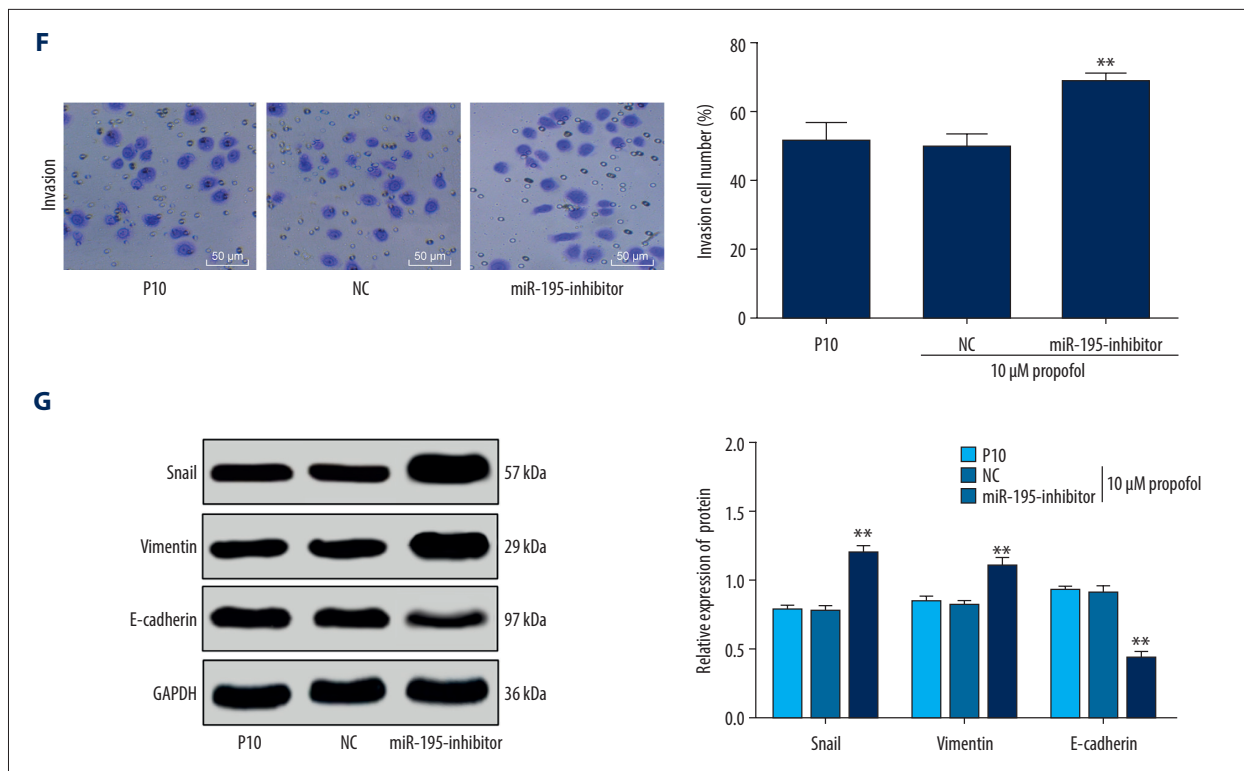
Figure 2. miR-195-5p is lowly-expressed in GC cells and downregulation of miR-195-5p reverses the effects of propofol treatment. (**A**) Differentially expressed miRNAs in SGC-7901 cells with or without propofol treatment evaluated using microarray analysis; (**B**) 5 miRNAs with most significant differential expression in SGC-7901 cells with or without propofol treatment measured using RT-qPCR. (**C**) Differential expression of miR-195-5p between GC tissues and normal tissues predicted via the online software (*http://starbase.sysu.edu.cn/panMirDiffExp.php*). (**D**) After miR-195-5p inhibitor transfection, miR-195-5p expression in SGC-7901 cells measured using RT-qPCR. (**E, F**) Migration (**E**) and invasion (**F**) of SGC-7901 cells detected using Transwell assays and observed under a microscope (200×). (**G**) Protein levels of Snail, vimentin and E-cadherin in SGC-7901 cells detected using western blot analysis. In panels **D**, **E**, and **F**, data were analyzed using one-way ANOVA, while in panels **B** and **G**, data were analyzed using 2-way ANOVA, and Tukey's multiple comparisons test was applied for post hoc test; compared to the NC group, * $P<0.05$, ** $P<0.01$; repetition=3. GC – gastric cancer; RT-qPCR – reverse transcription quantitative polymerase chain reaction; miR – microRNA; GAPDH – glyceraldehyde-3-phosphate dehydrogenase.

that miR-195-5p expression was decreased in GC tissues compared to the normal gastric tissues between the GC patients (n=372) and healthy individuals (n=32) ($P<0.01$) (Figure 2C).

We further transfected the propofol-treated cells with miR-195-5p inhibitor, and the transfection was successfully conducted according to RT-qPCR, since the miR-195-5p expression was notably reduced ($P<0.01$) (Figure 2D). miR-195-5p inhibition led to markedly elevated cell invasion and migration ($P<0.01$) (Figure 2E, 2F), elevated Snail and vimentin levels, while decreased E-cadherin level after 10 μM propofol treatment (all $P<0.01$) (Figure 2G).

miR-195-5p negatively targeted Snail

The miR-195-5p sequence was predicted to specifically bind to the 3'UTR of Snail (Figure 3A). miR-195-5p inhibition elevated the mRNA and protein levels of Snail in SGC-7901 cells pre-treated with 10 μM propofol (all $P<0.01$) (Figure 3B, 3C).

The bingding between miR-195-5p and Snail was further identified with luciferase assay, which showed the luciferase activity in cells co-transfected with miR-195-5p mimic and Snail 3'UTR WT plasmid significantly decreased ($P<0.01$), but that in cells co-transfected with miR-195-5p mimic and Snail 3'UTR MUT plasmid showed no major change (Figure 3D).

Upregulation of Snail reversed the effects of propofol treatment

The role of Snail in SGC-7901 cell invasion was identified as well. The 10 μM propofol-treated SGC-7901 cells were transfected with pcDNA3.1-Snail, after which the Snail expression significantly elevated ($P<0.01$) (Figure 4A, 4B). Upregulation of Snail increased the number of invaded and migrated cells ($P<0.01$) (Figure 4C, 4D), and it enhanced the Snail and vimentin protein levels but decreased the E-cadherin level in 10 μM propofol-treated SGC-7901 cells (all $P<0.01$) (Figure 4E).
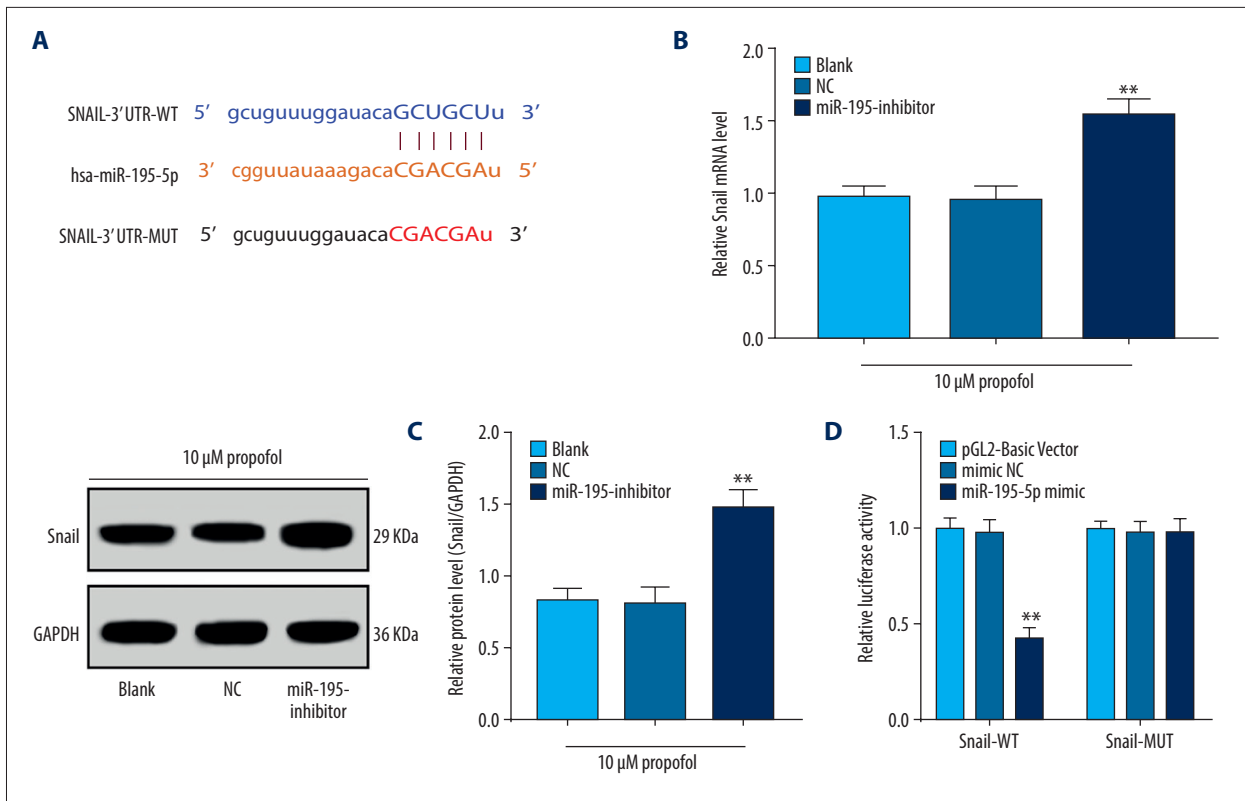
Figure 3. miR-195-5p negatively targets Snail. (**A**) Binding sites between miR-195-5p and Snail predicted via a computer-based program (*http://starbase.sysu.edu.cn/index.php*). (**B, C**) mRNA (**B**) and protein (**C**) expression of Snail following miR-195-5p inhibition detected using RT-qPCR and western blot analysis, respectively. (**D**) Target relation between miR-195-5p and Snail validated via luciferase assay. In panels **B** and **C**, data were analyzed using the *t*-test, *, compared to the NC group, * *P*<0.05, ** *P*<0.01; in panel **D**, data were analyzed using 2-way ANOVA, and Tukey's multiple comparisons test was applied for post hoc test; *, compared to the mimic NC group, * *P*<0.05, ** *P*<0.01; repetition=3.

Propofol suppressed tumor growth and metastasis *in vivo*

In vivo experiments were carried out to validate the findings *in vitro*. Compared to the control nude mice, the tumor volume and weight the propofol-treated mice reduced, and a higher propofol concentration led to further decreased tumor volume and weight (all *P*<0.01) (Figure 5A–5C). Besides, the tumor metastasis rates in liver and lung tissues were decreased following high dose of propofol treatment (Figure 5D).

Discussion

Most GC patients suffer from unpleasant prognosis because of the metastasis, which is caused by potent invasion and migration abilities of GC cells [23]. Propofol is a widely used anesthetic in the process of cancer resection surgery, and it has been recently recognized as a tumor inhibitor [24]. Propofol may exert functions though mediating miRNAs [13]. In this study, we probed the mechanisms of propofol in GC, with the findings that propofol inhibited GC cell metastasis

via elevating miR-195-5p expression and inhibiting Snail expression.

The initial finding of our study was that propofol treatment reduced the invaded and migrated SGC-7901 and NCI-N87 cell numbers. Emerging studies documented that propofol also presented anti-cancer functions, and in some cases by directly or indirectly inhibiting the metastasis of cancer cells. For instance, propofol has been proved to decrease the invasion and migration ability of human cholangiocarcinoma cells [25]. Likewise, it has been documented that propofol reduces migration of breast cancer cells via downregulating NET1 [26]. The same trends have also been found in GC, as propofol-based total intravenous anesthesia has been validated to improve the outcome and survival of GC patients who undergo surgical resection [27]. A previous study identified that propofol inhibits GC cell growth and invasion through downregulation of miR-221 [28]. Correspondingly, our study found that propofol treatment led to reduced protein levels of Snail and vimentin while elevated level of E-cadherin in GC cells. Over-expression of Snail and the following downregulation of
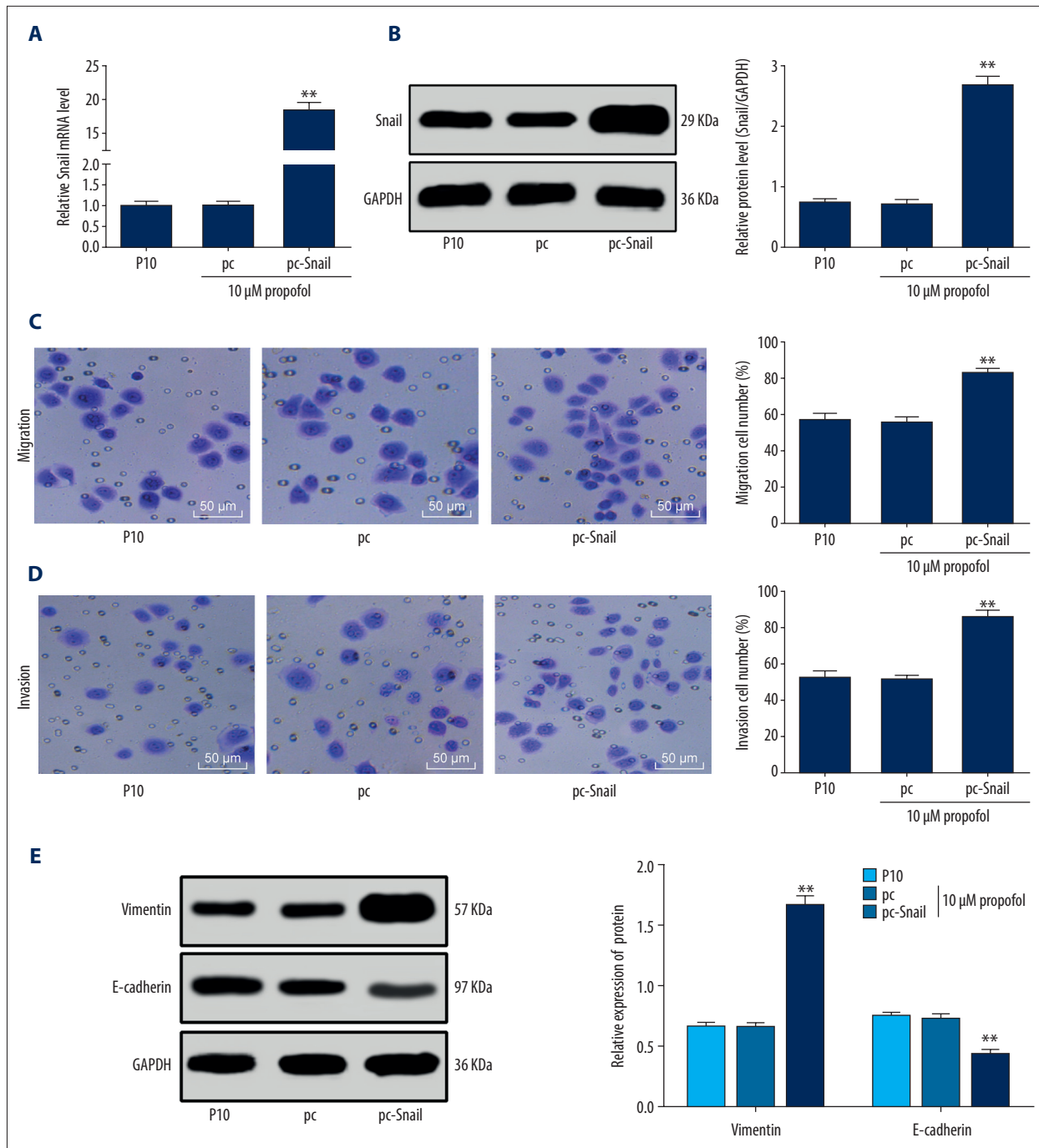
Figure 4. Upregulation of Snail promotes SGC-7901 cell invasion and migration. (**A, B**) mRNA (**A**) and protein (**B**) expression of Snail in SGC-7901 cells after pcDNA3.1-Snail transfection measured using RT-qPCR and western blot analysis, respectively. (**C, D**) Migration (**C**) and invasion (**D**) of SGC-7901 cells following Snail upregulation detected using Transwell assays and observed under a microscope (200×). (**E**) Protein levels of vimentin and E-cadherin in SGC-7901 cells following Snail upregulation determined using western blot analysis. In panel E, data were analyzed using 2-way ANOVA, while in the rest panels, data were analyzed using one-way ANOVA, and Tukey's multiple comparisons test was applied for post hoc test; compared to the pc group, * P<0.05, ** P<0.01; repetition=3. RT-qPCR – reverse transcription quantitative polymerase chain reaction.
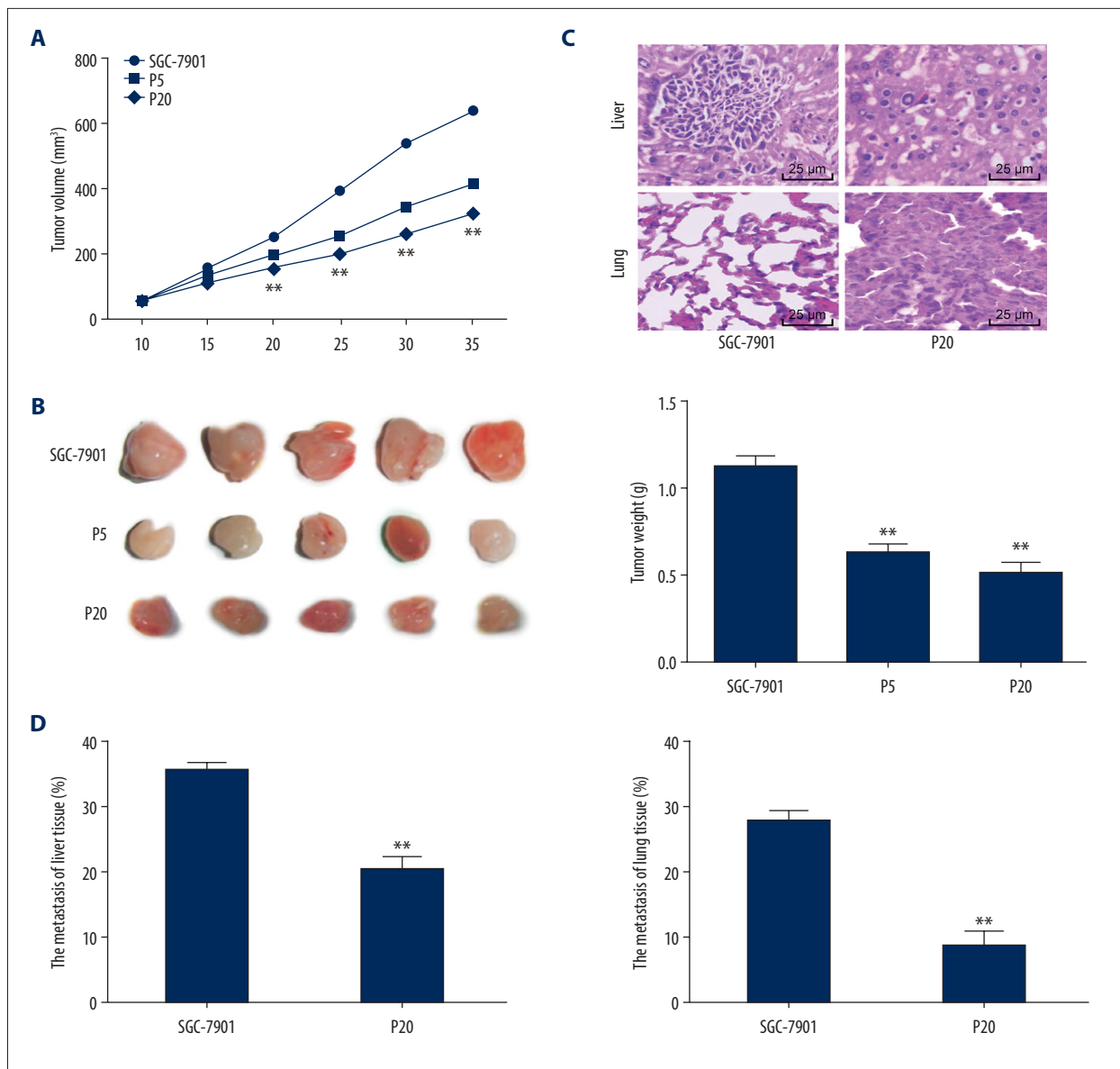
Figure 5. Propofol inhibits tumor growth and metastasis *in vivo*. (**A**) Tumor volume in each group of nude mice, n =5. (**B**) Observation of the resected tumors in each group of nude mice, n=5. (**C**) Tumor weight in each group of nude mice, n = 6. (**D**) Metastatic tumor in liver and lung tissues detected using H&E staining and observed under a microscope (400×), n=6. In panel **A**, data were analyzed using 2-way ANOVA, in panel **C**, data were analyzed using one-way ANOVA, while in panel **D**, data were analyzed using the *t*-test, and Tukey's multiple comparisons test was applied for post hoc test; * *P*<0.05, ** *P*<0.01.

E-cadherin occur during EMT, which is crucial for tumor invasion and distant metastasis [29]. Besides, vimentin is an important contributor for EMT via regulating its linked genes [30]. Similarly, propofol has been found to reduce vimentin and Snail expression, while increase E-cadherin expression, thus inhibiting EMT in lung cancer A549 cells [31]. These results further validated that propofol could reduce EMT in GC cells from the perspective of molecules.

Following the aforementioned findings, we measured the miRNAs with differential expression in SGC-7901 cells before and after propofol treatment using microarray analysis and RT-qPCR, which suggested that expression of miR-195-5p markedly elevated following propofol treatment. miR-195-5p has been recognized as a tumor inhibitor in several cancer types, and its dysregulation has been revealed to lead to chemo-resistance and unfavorable prognosis [17,32,33]. miR-195-5p has been found lowly expressed in GC patients, and the upregulation of miR-195-5p promoted GC cell death [34,35]. Likewise,

miR-195-5p has been documented to reduce GC cell invasion and migration and to suppress tumor formation in nude mice with xenograft tumor via downregulating basic fibroblast growth factor expression [36]. Quite in coincidence with our findings, miR-195 expression has been suggested to be elevated after propofol treatment, which inhibits the proliferation and metastasis of GC cells via the inactivation of the downstream signaling pathways [37]. Besides, our study identified that miR-195-5p intervention reversed the protective events of propofol in GC cells, which further validated that miR-195-5p was responsible for these events. Furthermore, we identified that miR-195-5p bound to the 3'UTR of Snail. Snail induces EMT partially by directly repressing E-cadherin transcription, during tumor progression and development, and low expression of E-cadherin is a marker of poor clinical outcomes [38]. As aforementioned, upregulation of Snail and downregulation of E-cadherin expression has been found in several cancers. Similarly, the vast majority of patients with progressive GC in a clinical-based study was found with aberrant Snail expression [39]. Reasonably, over-expression of Snail reversed the propofol-inhibited cell invasion in our study. Moreover, we found the *in vitro* results were reproduced in *in vivo* experiments where the volume and weight of xenograft tumor and the metastasis of tumor in nude mice were significantly reduced following propofol treatment. Collectively, it can be

inferred that propofol treatment inhibited GC invasion and migration both *in vivo* and *in vitro*.

Conclusions

To sum up, the current study provided evidence that propofol could suppress EMT, invasion and migration of GC cells via upregulation of miR-195-5p expression and the following downregulation of Snail. We hope these findings could offer novel insights for GC prevention and treatment. However, the findings were obtained from pre-clinical experiments. We hope more studies in this field would be carried out to validate our findings and to provide more evidence for the clinical practice of propofol application in GC treatment.

Availability of data and materials

The data that support the findings of this study are available from the corresponding author upon reasonable request.

Conflict of interest

None.

References:

1. Hassanalilou T, Ghavamzadeh S, Khalili L: Curcumin and gastric cancer: A review on mechanisms of action. J Gastrointest Cancer, 2019; 50(2): 185–92

2. Kinoshita H, Hayakawa Y, Koike K: Metaplasia in the stomach-precursor of gastric cancer? Int J Mol Sci, 2017; 18(10): pii: E2063

3. Guggenheim DE, Shah MA: Gastric cancer epidemiology and risk factors. J Surg Oncol, 2013; 107(3): 230–36

4. Wu JG, Wang JJ, Jiang X et al: MiR-125b promotes cell migration and invasion by targeting PPP1CA-Rb signal pathways in gastric cancer, resulting in a poor prognosis. Gastric Cancer, 2015; 18(4): 729–39

5. Fang XY, Pan HF, Leng RX, Ye DQ: Long noncoding RNAs: Novel insights into gastric cancer. Cancer Lett, 2015; 356(2 Pt B): 357–66

6. Wang R, Deng X, Yuan C et al: IFT80 improves invasion ability in gastric cancer cell line via ift80/p75NGFR/MMP9 signaling. Int J Mol Sci, 2018; 19(11): pii: E3616

7. Yoon JH, Choi WS, Kim O et al: Gastrokine 1 inhibits gastric cancer cell migration and invasion by downregulating RhoA expression. Gastric Cancer, 2017; 20(2): 274–85

8. Buschmann D, Brandes F, Lindemann A et al: Propofol and sevoflurane differentially impact microrRNAs in circulating extracellular vesicles during colorectal cancer resection: A pilot study. Anesthesiology, 2020; 132(1): 107–20

9. Jiang S, Liu Y, Huang L et al: Effects of propofol on cancer development and chemotherapy: Potential mechanisms. Eur J Pharmacol, 2018; 831: 46–51

10. Hemphill S, McMenamin L, Bellamy MC, Hopkins PM: Propofol infusion syndrome: A structured literature review and analysis of published case reports. Br J Anaesth, 2019; 122(4): 448–59

11. Cata JP, Owusu-Agyemang P, Kapoor R, Lonnqvist PA: Impact of anesthetics, analgesics, and perioperative blood transfusion in pediatric cancer patients: A comprehensive review of the literature. Anesth Analg, 2019; 129(6): 1653–65

12. Yang C, Gao J, Yan N et al: Propofol inhibits the growth and survival of gastric cancer cells *in vitro* through the upregulation of ING3. Oncol Rep, 2017; 37(1): 587–93

13. Ashrafizadeh M, Ezzati H, Ahmadi Z et al: Anti-tumor activity of propofol: A focus on microRNAs. Curr Cancer Drug Targets, 2019 [Epub ahead of print]

14. Alcantara KMM, Garcia RL: MicroRNA92a promotes cell proliferation, migration and survival by directly targeting the tumor suppressor gene NF2 in colorectal and lung cancer cells. Oncol Rep, 2019; 41(4): 2103–16

15. Karlsson S: Tipping clonal hematopoiesis into transformation. N Engl J Med, 2018; 379(3): 295–96

16. International BR: Expression of concern on "miR-195-5p suppresses the proliferation, migration, and invasion of oral squamous cell carcinoma by targeting TRIM14". Biomed Res Int, 2019; 2019: 8739375

17. Rezaei Z, Sebzari A, Kordi-Tamandani DM, Dastjerdi K: Involvement of the dysregulation of miR-23b-3p, miR-195-5p, miR-656-5p, and miR-340-5p in trastuzumab resistance of her2-positive breast cancer cells and system biology approach to predict their targets involved in resistance. DNA Cell Biol, 2019; 38(2): 184–92

18. Jolly MK, Celia-Terrassa T: Dynamics of phenotypic heterogeneity associated with EMT and stemness during cancer progression. J Clin Med 2019; 8(10): pii: E1542

19. Markopoulos GS, Roupakia E, Marcu KB, Kolettas E: Epigenetic regulation of inflammatory cytokine-induced epithelial-to-mesenchymal cell transition and cancer stem cell generation. Cells, 2019; 8(10): pii: E1143

20. Paolillo M, Schinelli S: Extracellular matrix alterations in metastatic processes. Int J Mol Sci, 2019; 20(19): pii: E4947

21. Zhang HY, Li CH, Wang XC et al: MiR-199 inhibits EMT and invasion of hepatoma cells through inhibition of Snail expression. Eur Rev Med Pharmacol Sci, 2019; 23(18): 7884–91

22. Chen X, Li J, Hu L et al: The clinical significance of snail protein expression in gastric cancer: A meta-analysis. Hum Genomics, 2016; 10(Suppl. 2): 22

23. Tan BB, Li Y, Fan LQ et al: Upregulated Vav2 in gastric cancer tissues promotes tumor invasion and metastasis. Tumour Biol, 2017; 39(5): 1010428317698392

24. Sun H, Gao D: Propofol suppresses growth, migration and invasion of A549 cells by down-regulation of miR-372. BMC Cancer, 2018; 18(1): 1252

25. Zhang Z, Zang M, Wang S, Wang C: Effects of propofol on human cholangiocarcinoma and the associated mechanisms. Exp Ther Med, 2019; 17(1): 472–78

26. Ecimovic P, Murray D, Doran P, Buggy DJ: Propofol and bupivacaine in breast cancer cell function *in vitro* – role of the NET1 gene. Anticancer Res, 2014; 34(3): 1321–31

27. Zheng X, Wang Y, Dong L et al: Effects of propofol-based total intravenous anesthesia on gastric cancer: A retrospective study. Onco Targets Ther, 2018; 11: 1141–48

28. Wang ZT, Gong HY, Zheng F et al: Propofol suppresses proliferation and invasion of gastric cancer cells via downregulation of microRNA-221 expression. Genet Mol Res, 2015; 14(3): 8117–24

29. Palma Cde S, Grassi ML, Thome CH et al: Proteomic analysis of epithelial to mesenchymal transition (EMT) reveals cross-talk between SNAIL and HDAC1 proteins in breast cancer cells. Mol Cell Proteomics, 2016; 15(3): 906–17

30. Ivaska J: Vimentin: central hub in EMT induction? Small GTPases, 2011; 2(1): 51–53

31. Liu WZ, Liu N: Propofol inhibits lung cancer A549 cell growth and epithelial-mesenchymal transition process by upregulation of microRNA-1284. Oncol Res, 2018; 27(1): 1–8

32. Feng C, Zhang L, Sun Y et al: GDPD5, a target of miR-195-5p, is associated with metastasis and chemoresistance in colorectal cancer. Biomed Pharmacother, 2018; 101: 945–52

33. Jin Y, Wang M, Hu H et al: Overcoming stemness and chemoresistance in colorectal cancer through miR-195-5p-modulated inhibition of notch signaling. Int J Biol Macromol, 2018; 117: 445–53

34. Gorlewicz JL, Battaglia S, Smith BF et al: Wireless insufflation of the gastrointestinal tract. IEEE Trans Biomed Eng, 2013; 60(5): 1225–33

35. Zhao DL, Wu QL: Effect of inhibition to Yes-related proteins-mediated Wnt/beta-catenin signaling pathway through miR-195-5p on apoptosis of gastric cancer cells. Eur Rev Med Pharmacol Sci, 2019; 23(15): 6486–96

36. Wang J, Li L, Jiang M, Li Y: MicroRNA-195 inhibits human gastric cancer by directly targeting basic fibroblast growth factor. Clin Transl Oncol, 2017; 19(11): 1320–28

37. Zhang W, Wang Y, Zhu Z et al: Propofol inhibits proliferation, migration and invasion of gastric cancer cells by up-regulating microRNA-195. Int J Biol Macromol, 2018; 120(Pt A): 975–84

38. Barrallo-Gimeno A, Nieto MA: The Snail genes as inducers of cell movement and survival: Implications in development and cancer. Development, 2005; 132(14): 3151–61

39. Wang ZS, Shen Y, Li X et al: Significance and prognostic value of Gli-1 and Snail/E-cadherin expression in progressive gastric cancer. Tumour Biol, 2014; 35(2): 1357–63